Supporting Information

Kinetics of Asymmetric Transfer Hydrogenation, Catalyst Deactivation, and Inhibition with Noyori Complexes as Revealed by Real-time High Resolution FlowNMR Spectroscopy

Andrew M. R. Hall,[a,b] Peilong Dong,[c] Anna Codina,[d] John P. Lowe,[b,c] Ulrich Hintermair[a,b*]

[a] Centre for Sustainable Chemical Technologies, University of Bath, Bath BA2 7AY, United Kingdom.
[b] Dynamic Reaction Monitoring Facility, University of Bath, Bath BA2 7AY, United Kingdom.
[c] Department of Chemistry, University of Bath, Bath BA2 7AY, United Kingdom.
[d] Bruker UK, Banner Lane, Coventry CV4 9GH, United Kingdom.
[*] **Corresponding author:** U.Hintermair@bath.ac.uk

Table of Contents

***Table S1**: Conversion data for transfer hydrogenation of acetophenone performed under inert atmosphere (Schlenk tube, Ar atmosphere) and with the reaction vessel exposed to air. (0.4 M acetophenone, 0.01 M KOH, 9.5 mL dry isopropanol, 2 mM (**1**), 0.1 M 1,3,5-trimethoxybenzene (internal concentration reference), 20°C).*

Catalyst concentration (mM)	Reaction time (h)	Conversion under air	Conversion under inert atmosphere
4	2	84%	90%
2	4	80%	88%
1	6	67%	87%

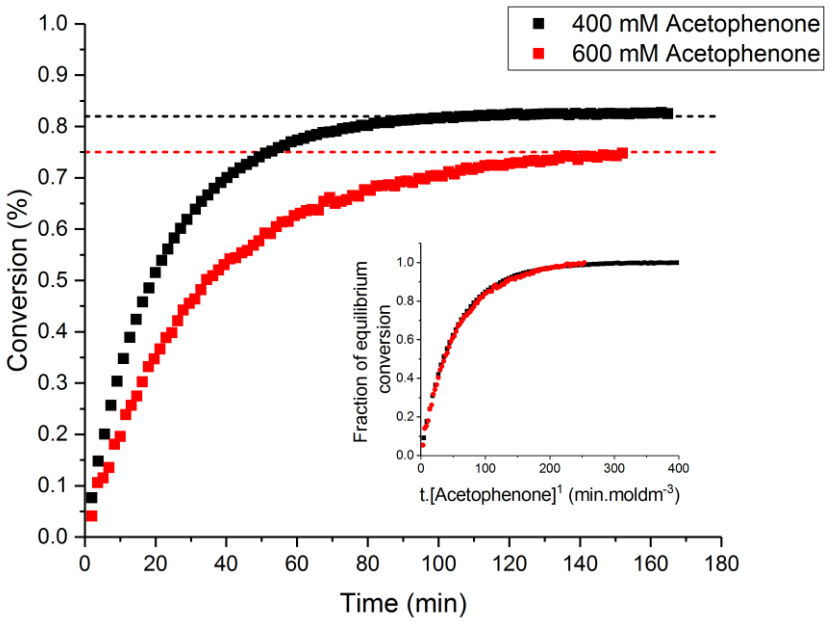

***Figure S1**: Conversion plots for the catalytic transfer hydrogenation of acetophenone with various amounts of substrate (2 mM **(1)**, 10 mM KOH, 9.5 mL dry isopropanol, 20°C), showing dependence of acetophenone concentration on reaction rate. Inset: Variable Time Normalisation Analysis (VTNA) of conversion data, normalised for different equilibrium position due to change in reaction conditions, showing first order dependence of reaction rate on acetophenone concentration.*

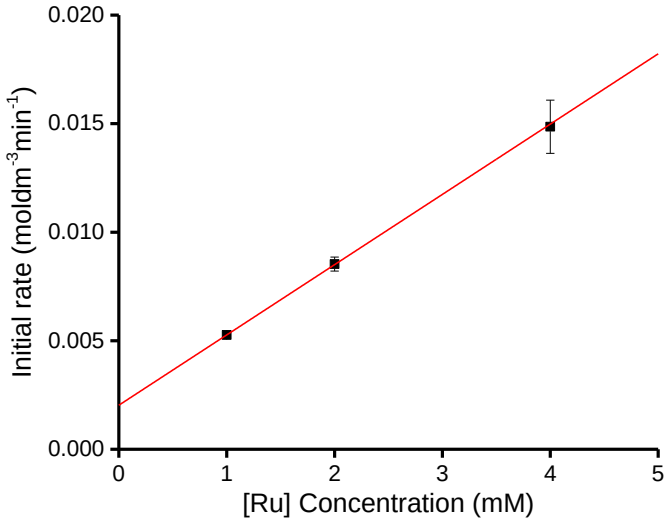

***Figure S2**: Initial rate data for the asymmetric transfer hydrogenation of acetophenone catalysed by the Noyori catalyst, (R,R)-**1**, (0.4 M acetophenone, 0.01 M KOH, 9.5 mL dry isopropanol, 0.1 M 1,3,5-trimethoxybenzene (internal concentration reference), 25°C), showing first order dependence of catalyst concentration on reaction rate.*

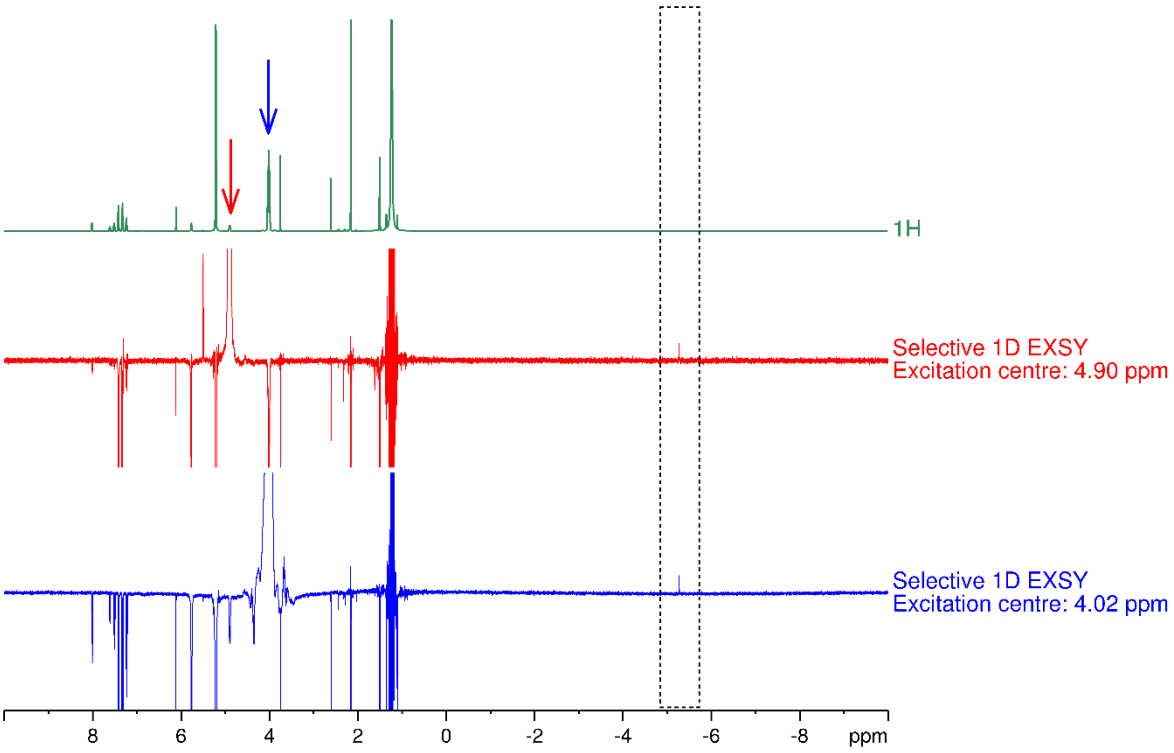

***Figure S3**: Selective 1D EXSY NMR data showing excitation of isopropanol and 1-phenylethanol alcohol CH peaks, and the resulting exchange signal (-5.3 ppm) attributed to **(3)**. Negative peaks are NOESY interactions of isopropanol and 1-phenylethanol respectively. (0.8 M acetophenone, 0.01 M KOH, 0.5 mL dry isopropanol, 20 mM **(1)**, 0.1 M 1,3,5-trimethoxybenzene (internal concentration reference), 25°C). Selective NOESY with gradient refocusing (128 scans, 2.18 s acquisition time, 2 s delay time, 80000 µs Gaussian excitation peak, 0.5 s mixing time).*

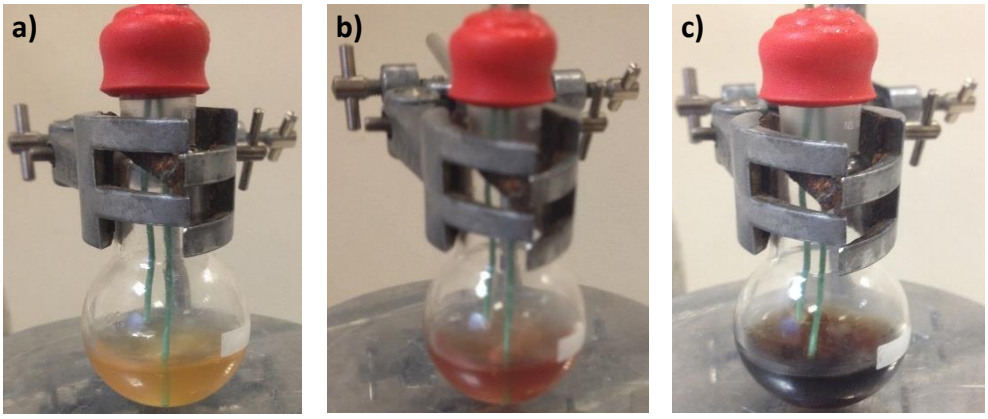

***Figure S4**: Photographs of a) **(1)** dissolved in 0.01 M KOH solution in isopropanol, b) **(1)** dissolved in 0.01 M KOH solution in isopropanol with 0.4 M acetophenone added, c) **(1)** dissolved in 0.01 M KOH solution in isopropanol with 0.4 M acetophenone added after exposure to air.*

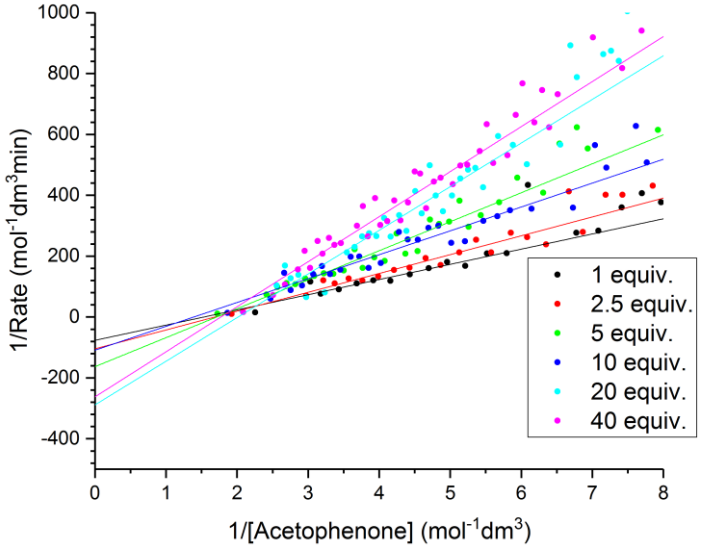

***Figure S5**: Lineweaver-Burk analysis of catalytic transfer hydrogenation of acetophenone (400 mM acetophenone, 2 mM **(1)**, 9.5 mL dry isopropanol, 0.1 M 1,3,5-trimethoxybenzene (internal concentration reference), 20°C) with varying equivalents of KOH per [Ru] (1 scan, 1.64 s acquisition time, 1 s relaxation delay time).*

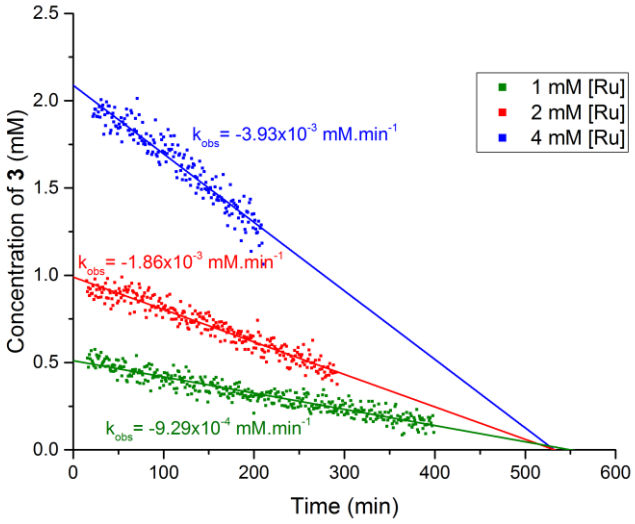

***Figure S6**: Concentration profiles of the hydride peak at -5.3 ppm attributed to **(3)** during the course of catalytic transfer hydrogenation reaction of acetophenone to 1-phenylethanol in flow at 4 mL/min (400 mM acetophenone, 10 mM KOH, 9.5 mL dry isopropanol, 0.1 M 1,3,5-trimethoxybenzene (internal concentration reference), 20°C), showing first order deactivation of **(3)** at varying catalyst loadings. Selective excitation of **(3)** using a gradient spin echo pulse sequence with a shaped 180° pulse centred on the hydride peak (20°C, 24 scans, 1 s acquisition time, 1 s delay time, 880 µs Gaussian shaped pulse).*

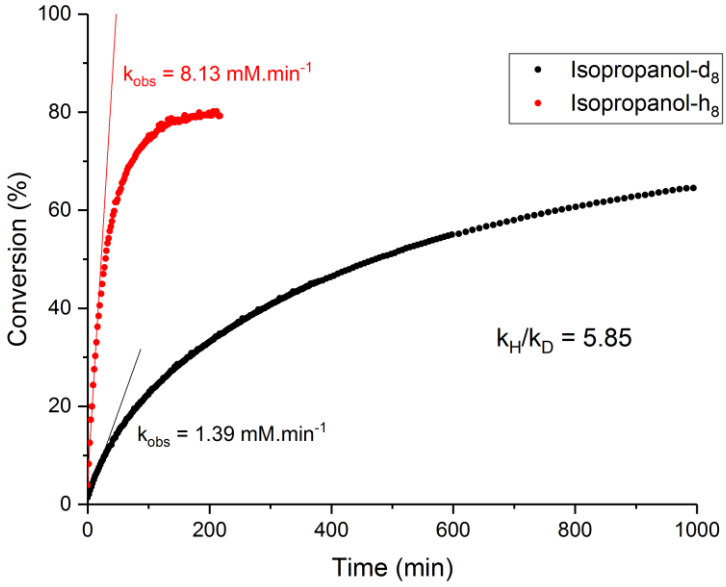

***Figure S7**: Kinetic data for transfer hydrogenation reaction of acetophenone perfromed in isopropanol-h_8 or isopropanol-d_8 demonstrating a strong kinetic isotope effect of 5.85, (0.4 M acetophenone, 0.02 M KOH, 9.5 mL isopropanol, 2 mM **(1)**, 0.1 M 1,3,5-trimethoxybenzene (internal concentration reference), 20°C). Selective excitation using spin echo shaped pulse sequence (8 scans, 2 s acquisition time, 1 s delay time, 1600 µs Gaussian excitation peak).*

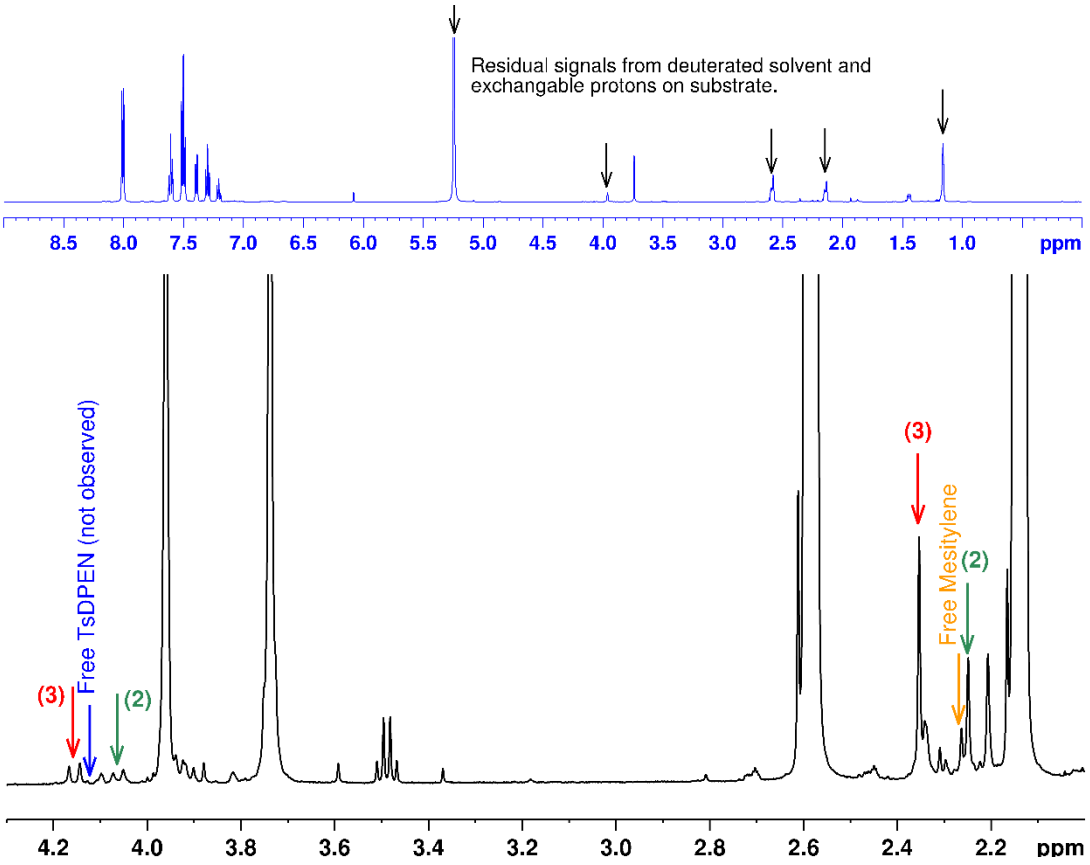

***Figure S8**: Sample spectrum for the catalytic transfer hydrogenation reaction of acetophenone in flow at 2 mL/min, showing the position of TsDPEN and mesitylene peaks of **(2)** + **(3)**, along with free TsDPEN and free mesitylene as determined by spiking reaction mixture (2 mM **(1)**, 400 mM acetophenone, 20 mM KOD, 9.5 mL isopropanol-d_8, 20°C, 16 scans, 1.64 s acquisition time, 1 s delay time).*

Experimental

FlowNMR apparatus

Reactions were carried out in a standard glass round-bottomed flask, with a double-piston HPLC pump (JASCO PU-2085 Plus) with a semi-micro pump head used to circulate the mixture around the system to an InsightMR flow tube (Bruker) located within the spectrometer (Bruker 400 or 500 MHz Avance II+ Ultrashield equipped with either a broadband (BBO) probe or a nitrogen cooled Prodigy CryoProbe). In order to minimise the delay time between a change occurring in the reaction vessel and the arrival of the sample to the spectrometer for detection it is desirable to ensure that the volume of the tubing connecting the reaction vessel to the spectrometer is minimised, therefore narrow diameter polyetheretherketone (PEEK) tubing (0.762 mm i.d., Upchurch Scientific) was used. The PEEK tubing offers high chemical and mechanical stability (pH 0 – 14, -50 – 100 °C, >300 bar) along with good flexibility and low gas permeability. For reactions at atmospheric pressure standard rubber seals were used to connect the tubing with the reaction solution, and were found to be effective for air-sensitive systems over prolonged times (>10 hours) when sealed off with silicone grease.

The total volume of the flow apparatus was 3.7 mL, and the volume of the NMR flow cell was approximately 0.5 mL, corresponding to a mean residence time within the detection region of 8 seconds at a flow rate of 4 $mLmin^{-1}$.[1]

All other connections were made using standard HPLC-type PEEK connectors (Upchurch Scientific), allowing the apparatus to be purged with inert or reactive gases as required. All equipment was positioned on a mobile trolley made of plastic (Rubbermaid), allowing the equipment to be transported between the laboratory and the spectrometer as required. The trolley and apparatus were able to be placed at a minimum distance of 0.5 m from the shielded magnet without experiencing adverse magnetic effects.

Data acquisition was performed without lock and with shimming performed using automated ^{1}H shimming routines, followed by manual fine tuning. Data processing was performed using commercially available software.

All samples were prepared using reagents and catalyst purchased from Sigma Aldrich or Alfa Aesar at reagent grade or higher. Acetophenone was distilled and isopropanol degassed prior to use. All other reagents were used without further purification.

Receiver Gain calibration

Since selective excitation experiments are recorded at significantly higher receiver gain than standard proton spectra, it is necessary to determine a compensation factor to allow quantitative comparison between peaks on the two different spectra.

Relative integral area of the methyl peak of a 100 $mgdm^{-3}$ solution of 1,3,5-trimethoxybenzene solution in isopropanol were recorded at a range of receiver gains, resulting in a calibration factor of 1.033 to transform integral values recorded at different receiver gains.

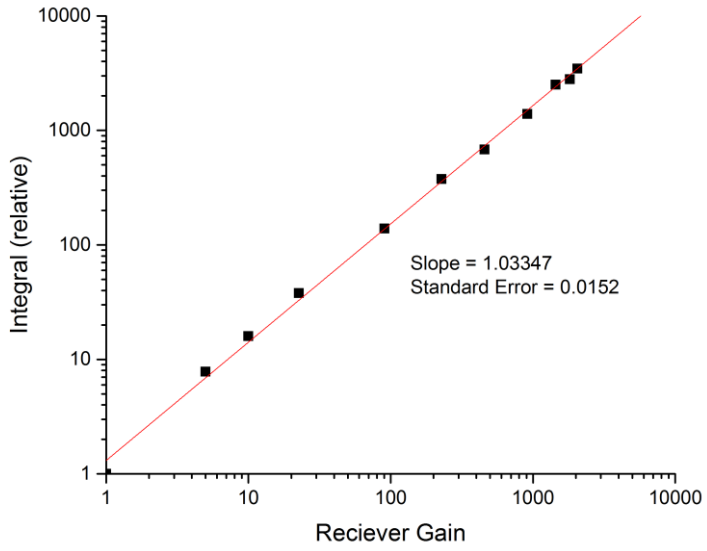

***Figure S9**: Receiver gain calibration for Bruker 500 MHz Avance II+ Ultrashield spectrometer with broadband BBO probe. 100 $mgdm^{-3}$ 1,3,5-trimethoxybenzene in isopropanol calibration standard. Selective excitation using spin echo shaped pulse sequence (8 scans, 2 s acquisition time, 1 s delay time, 1600 µs Gaussian excitation peak, 20°C).*

In order to allow comparison between the integral of the hydride peak recorded using selective excitation and the 1,3,5-trimethoxybenzene concentration reference, the integral of the hydride peak is reduced to give a Reduced Integral Value (RIV) according to the following equation:

Equation 1: $$RIV = \frac{I_{hydride} \times RG_{normal} \times 1.033}{RG_{hydride}}$$

Where $I_{hydride}$ = Integral area of hydride peak, RG_{normal} = receiver gain for selective excitation experiment of internal standard (e.g. TMB), $RG_{hydride}$ = receiver gain for selective excitation experiment of hydride.

The concentration of the hydride species can then be calculated by comparison to a selective excitation experiment of the internal reference (such as 1,3,5-trimethoxybenzene (TMB)) of known concentration:

Equation 2: $$[Hydride] = RIV \times \frac{[TMB]}{I_{TMB}/Number\ of\ protons\ associated\ with\ TMB\ peak}$$

This calculation process was tested on a standard sample containing known concentrations of acetophenone and 1,3,5-trimethoxybenzene in isopropanol solvent and the accuracy of component concentrations calculated with this method compared to actual concentrations of components was found to have an error 3.6%.

NMR acquisition parameters

Unless specified in figure captions, the following parameters were used for the acquisition of all NMR data:

^{1}H selective excitation and ^{1}H (non-selective) spectra acquisition were interleaved with selective excitation spectra acquired every 30 seconds and non-selective spectra acquired every 60 seconds.

^{1}H (without selective excitation)

^{1}H spectra for the determination 1-phenylethanol, acetophenone, acetone and 1,3,5-trimethoxybenzene concentration were acquired using a standard 30° pulse sequence, with a 1.64 s acquisition time and 1 s relaxation delay time, using a single transient.

^{1}H Selective excitation

^{1}H selective excitation spectra for the determination of the concentration of catalyst species **3** were acquired using a 1D double spin echo pulse sequence with gradient refocusing. A Q3 gaussian 180° pulse with a pulse length of 2272 µs (approximately 3 ppm width), centred on -5.5 ppm was used for selective refocusing with a 200 µs gradient recovery time. 8 transients were acquired with a 2 s acquisition time and 1 s relaxation delay time.

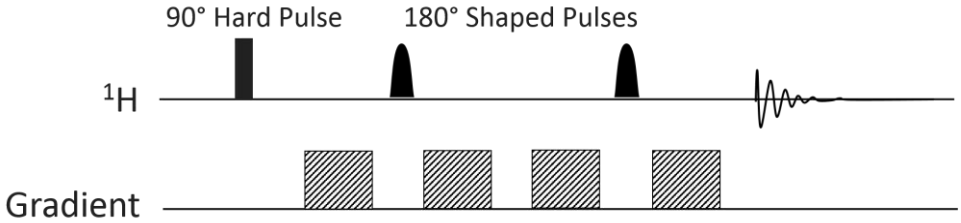

***Figure S10**: Schematic illustration of double spin echo pulse sequence with gradient refocusing*

^{1}H EXSY

^{1}H selective exchange spectroscopy (EXSY) spectra were carried out with a 1D spin echo pulse sequence with gradient refocusing using a gaussian shaped selective 180° pulse with a length of 80 ms, centred on either 4.90 or 4.02 ppm. 128 transients were acquired with 2.18 s acquisition time, 2 s relaxation delay time and 0.5 s NOESY mixing time.

Transfer hydrogenation of acetophenone

The FlowNMR apparatus was purged with dry nitrogen for 30 min to remove any traces or air or moisture. The apparatus was filled with 8.53 mL of a stock solution of potassium hydroxide (anhydrous, 0.112 g, 2 mmol) and 1,3,5-trimethoxybenzene (3.364 g, 0.02 mol) in dry, degassed isopropanol (200 mL).

The flow tube was then inserted into the spectrometer and automated shimming and tuning routines were performed. Best results were obtained if automated shimming and tuning was performed on static samples, however acceptable results were still obtained in flow. Frequency lock was switched off when using non-deuterated solvents, and shimming performed on proton peaks. Manual fine tuning of X and Y shims was often required to get a good peak line width. Spectra of the reagents were recorded without flow and again at the flowrate desired for the reaction. Comparison of the integral area of the peaks in each spectrum was used to calculate a correction factor for each reagent peak. (I = peak integral, CF = correction factor).[1]

Equation 3: $$I_{Corrected} = CF \times I$$

Equation 4: $$CF = \frac{I_{Static}}{I_{Flow}}$$

With the sample flowing, data acquisition was started using an automated kinetic routine or dedicated reaction monitoring software, with spectra recorded at specified time intervals. (4 s delay, 1.64 s acquisition time, 30° pulse, 4 scans) and a concentrated solution of the catalyst (*R,R*)-(TsDPEN)mesitylruthenium chloride (12 mg, 0.02 mmol) dissolved in 1 mL of the stock solution was added. To start the reaction, acetophenone (0.47 mL, 4 mmol) was added.

At the end of the reaction, or if intermediates of interest were observed, additional spectra were recorded with and without flow, and correction factors were calculated for the intermediate or product peaks, which were applied to each spectrum to give the final peak areas for calculation of species concentration and plotting of kinetic data.

Concentrations of species were determined by peak integrals and referenced to 1,3,5-trimethoxybenzene internal standard.

For the reverse reaction (Figure 4a), acetophenone was substituted with racemic 1-phenylethanol (0.47 mL, 4 mmol) and isopropanol was substituted with acetone (9.5 mL). For the catalyst stability test (Figure 4b), additional acetophenone (0.47 mL, 4 mmol) was added after 100 minutes. For

experiments with varying concentration of base, acetophenone or catalyst, the above method was adjusted with the appropriate quantities of each reagent.

Kinetic Isotope Effect (KIE) and deactivation studies (Figures 13 and S7) were performed using the method described above, with isopropanol replaced with perdeuterated-isopropanol and potassium hydroxide replaced with potassium deuteroxide.

EXSY data (Figure S8) was acquired on a sample of **1** (4.6 mg, 0.0074 mmol) and acetophenone (0.05 mL, 0.4 mmol) in 0.5 mL of a stock solution containing 1,3,5-trimethoxybenzene (0.1 M) and potassium hydroxide (0.01 M) in isopropanol (non-deuterated).

Catalyst Intermediate Synthesis[4]

Unsaturated intermediate (2)

Noyori catalyst (80 mg, 0.13 mmol) was dissolved in dry DCM (5 mL) to give a bright orange solution. A solution of potassium tert-butoxide (0.13 mL, 1M in THF, 0.13 mmol) was added, causing the solution to immediately turn deep purple in colour. The mixture was stirred for 5 mins at room temperature before filtering. The purple filtrate was evaporated under vacuum and the resulting purple solid dried overnight under vacuum to give a purple powder: Isolated yield: 0.029 g, 36%. λ_{max} = 565 nm, ϵ_{565} = 1377 $mol^{-1}dm^3cm^{-1}$.

Hydride intermediate (3)

Unsaturated intermediate was dissolved in dry isopropanol (5 mL) to give a yellow-brown solution. Solvent was evaporated under vacuum to give a brown powder. ^{1}H NMR (400 MHz) δ ($CDCl_3$): -5.5 (s, 1H).

Chiral separation of enantiomers

HPLC analysis carried out using an Agilent 1260 Infinity II LC instrument fitted with a Chiracell OD-H column (Daicell chiral, 250 mm length, 4.6 mm diameter, 5 µm particule size). Samples were eluted with a 9:1 Hexane:IPA solvent mixture at 1 mL/min with detection using a UV detector at 254 nm. The (R)-1-phenylethanol peak was observed after 7.6 minutes, and (S)-1-phenylethanol at 8.2 minutes. Enantiomeric excesses were calculated using Equation 5:

Equation 5: $$\%ee = \frac{[S]-[R]}{[S]+[R]} \times 100$$

Kinetic Modelling

Qualitative kinetic modelling was performed with COPASI 4.15 Biochemical modelling software, using a deterministic (LSODA) time course model (10000 s duration, 1 s time interval).[2] Reaction parameters were taken from our experimental conditions and rate law expressions as derived below. Since individual rates of elementary reaction steps are not known, values for the kinetic parameters were chosen to qualitatively provide a good visual fit with experimental data. The purpose of the kinetic model is to assess the viability of the proposed mechanism by comparison of experimental and simulated trends, and kinetic parameters do not necessarily represent true reaction rates.

Species and starting concentrations:

Species	Starting Concentration (mmol/mL)
Propan-2-ol	12.64
Acetone	0
Acetophenone	0.4
1-phenylethanol	0
KOH	0.02
1	0.002
2	0
3	0
4	0
5	0

Reactions:

1	**1** + KOH -> **2**	irreversible	k_1
2	**2** + Propan-2-ol = **3** + Acetone	reversible	k_2, k_{-2}
3	**3** + Acetophenone = **2** + 1-phenylethanol	reversible	k_3, k_{-3}
4	**2** + KOH = **4**	reversible	k_4, k_{-4}
5	**3** -> **5**	irreversible	k_5

Events:

Time = 600 s	Catalyst **1** added
Time = 1200 s	Acetophenone added

Kinetic parameters:

k_1	1000	mL/(mmol*s)
k_2	1	mL/(mmol*s)
k_{-2}	0.032	mL/(mmol*s)
k_3	1	mL/(mmol*s)
k_{-3}	0.168	mL/(mmol*s)
k_4	1	mL/(mmol*s)
k_{-4}	0.1	1/s
k_5	0.0001	1/s

Acetophenone concentration variation

To simulate the effect of varying concentration of acetophenone, the model was run using starting concentrations of acetophenone between 0.2 and 1 moldm^{-3}. All other parameters were identical to those described above. The simulated curves reproduce the trend observed experimentally in Figure S1, including the change in equilibrium conversion.

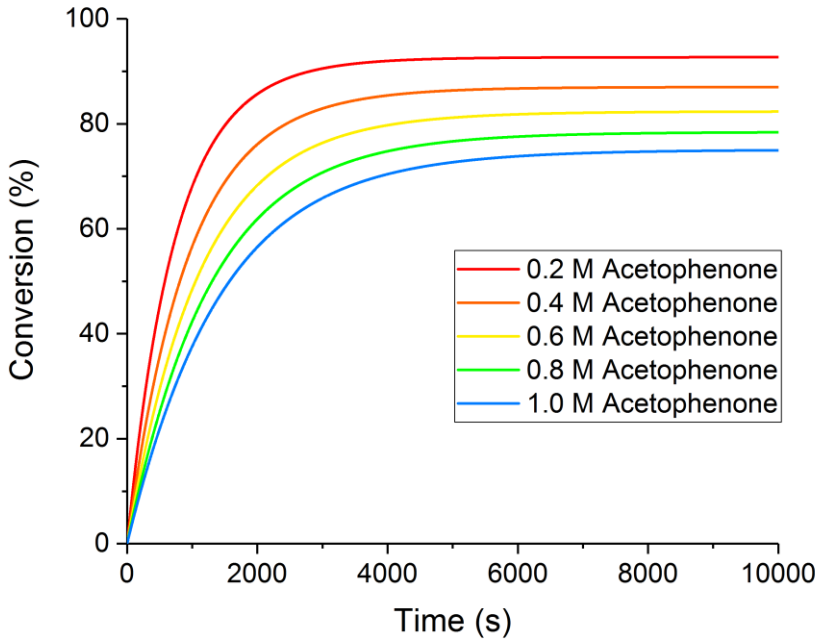

***Figure S11**: Simulated reaction kinetics for proposed mechanism of the catalytic transfer hydrogenation of acetophenone to 1-phenylethanol, showing the effect of acetophenone concentration on the reaction rate and equilibrium conversion.*

Catalyst concentration variation

To simulate the effect of varying concentration of catalyst, the model was run using starting concentrations of ruthenium chloride complex **(1)** between 0.001 and 0.005 moldm^{-3}. All other parameters were identical to those described above. The simulated curves reproduce the trends observed experimentally in Figures 3 and S6, including change in reaction rate and catalyst deactivation rate.

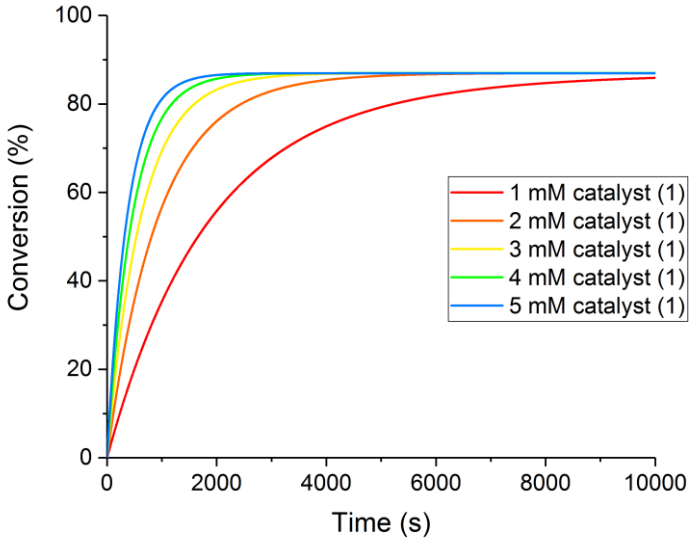

***Figure S12**: Simulated reaction kinetics for proposed mechanism of the catalytic transfer hydrogenation of acetophenone to 1-phenylethanol, showing the effect of catalyst concentration on the reaction rate.*

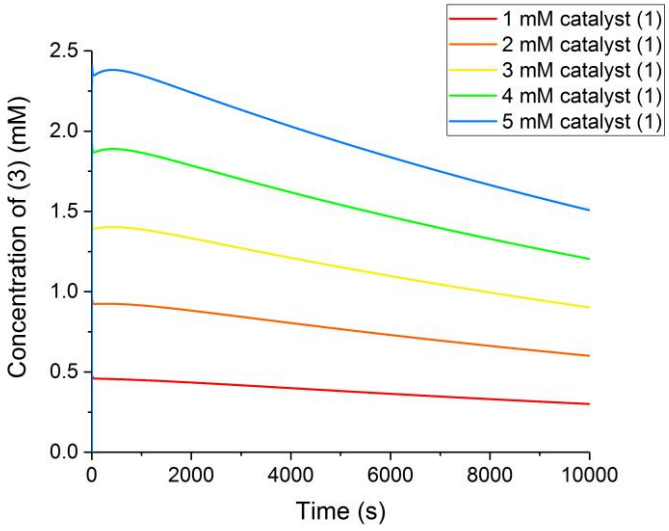

***Figure S13**: Simulated reaction kinetics for proposed mechanism of the catalytic transfer hydrogenation of acetophenone to 1-phenylethanol, showing the effect of catalyst concentration on the concentration of hydride **(3)** present during turnover, and deactivation rate.*

Modelling of enantiomeric excess

To assess the effect of catalytic turnover on the enantioselectivity of the product, the model was repeated with additional terms for (*R*) and (*S*)-1-phenylethanol. The 98.5 : 1.5 ratio of reaction rates for (*R*) and (*S*) product was determined using the predicted enantioselectivity of the reaction reported from DFT calculations of the transition states.[3]

Species and starting concentrations:

Species	Starting Concentration (mmol/mL)
Propan-2-ol	12.64
Acetone	0
Acetophenone	0.4
(R)-1-phenylethanol	0
(S)-1-phenylethanol	0
KOH	0.02
1	0.002
2	0
3	0
4	0
5	0

Reactions:

1	**1** + KOH -> **2**	irreversible	k_1
2	**2** + Propan-2-ol = **3** + Acetone	reversible	k_2, k_{-2}
3R	**3** + Acetophenone = **2** + (R)-1-phenylethanol	reversible	k_{3R}, k_{-3R}
3S	**3** + Acetophenone = **2** + (S)-1-phenylethanol	reversible	k_{3S}, k_{-3S}
4	**2** + KOH = **4**	reversible	k_4, k_{-4}
5	**3** -> **5**	irreversible	k_5

Events:

Time = 600 s	Catalyst **1** added
Time = 1200 s	Acetophenone added

Kinetic parameters:

k_1	1000	mL/(mmol*s)
k_2	1	mL/(mmol*s)
k_{-2}	0.032	mL/(mmol*s)
k_{3R}	0.985	mL/(mmol*s)
k_{-3R}	0.165	mL/(mmol*s)
k_{3S}	0.015	mL/(mmol*s)
k_{-3S}	0.003	mL/(mmol*s)
k_4	1	mL/(mmol*s)
k_{-4}	0.1	1/s
k_5	0.0001	1/s

The simulated enantioselectivity plot starts at a maximum enantioselectivity of 97% and slowly decreases over the course of the reaction due to the reversible reaction and the cumulative effect of the enantioselectivity of the elementary reaction steps. Both the initial enantioselectivity and the subsequent decline match the experimentally observed data (Figure 2) well.

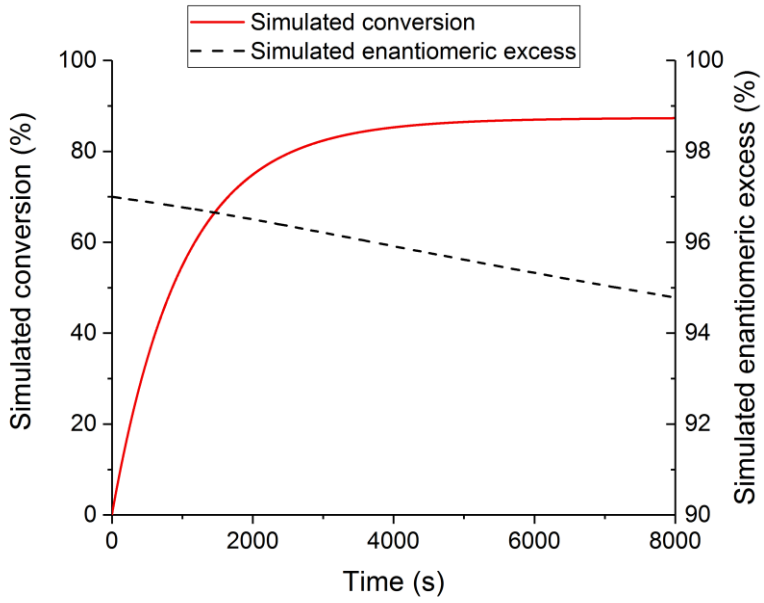

***Figure S14**: Simulated reaction kinetics for proposed mechanism of the catalytic transfer hydrogenation of acetophenone to (R) or (S)-1-phenylethanol along with change in enantioselectivity during course of reaction.*

Rate law derivation

Simple mechanism

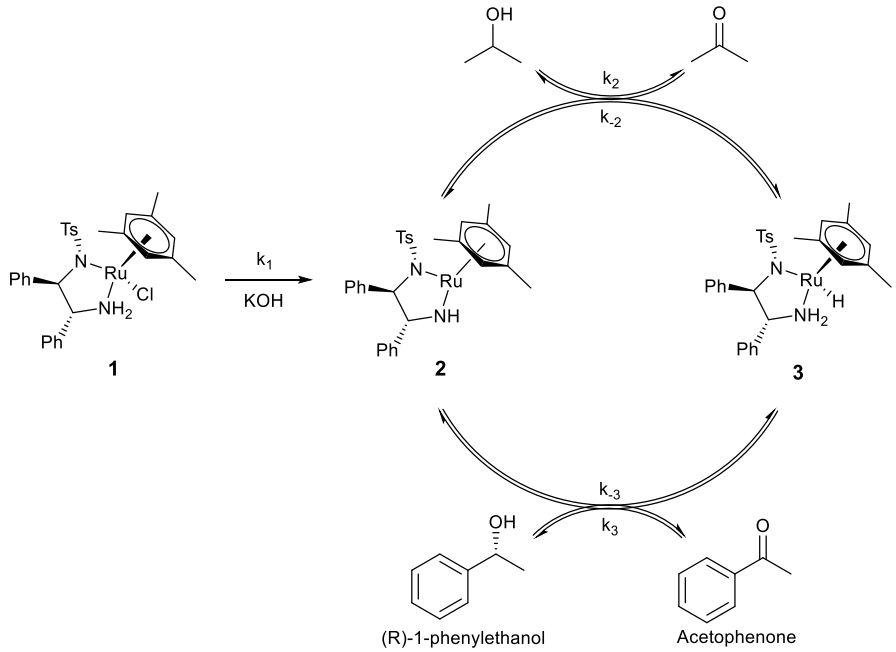

Assumptions:

- $k_1 \gg k_2$, k_{-2}, k_3, k_{-3}, therefore can be neglected and [**1**]≈0
- Steady State Approximation

From the mechanism:

Equation A: $$rate = \frac{d[PE]}{dt} = k_3[3][Acp] - k_{-3}[2][PE]$$

Equation B: $$\frac{d[2]}{dt} = -k_2[2][IPA] + k_{-2}[3][Ac] + k_3[3][Acp] - k_{-3}[2][PE] \cong 0$$

Equation C: $$[Ru] \cong [2] + [3]$$

Rearranging Eq. B: $$k_2[2][IPA] + k_{-3}[2][PE] = k_{-2}[3][Ac] + k_3[3][Acp]$$

$$\frac{[2]}{[3]} = \frac{k_{-2}[Ac]+k_3[Acp]}{k_2[IPA]+k_{-3}[PE]} = K_{cat}$$ [Equation D]

Combining Eq. C + D: $$[Ru] = K_{cat}[3] + [3] = (K_{cat} + 1)[3]$$

$$[3] = \frac{[Ru]}{(K_{cat}+1)}$$ [Equation E]

Combining Eq. A + D: $$rate = k_3[3][Acp] - k_{-3}[3][PE]K_{cat}$$

$$= (k_3[Acp] - k_{-3}[PE]K_{cat})[3]$$

$$\boxed{rate = (k_3[Acp] - k_{-3}[PE]K_{cat})\frac{[Ru]}{(K_{cat} + 1)}}$$

With deactivation

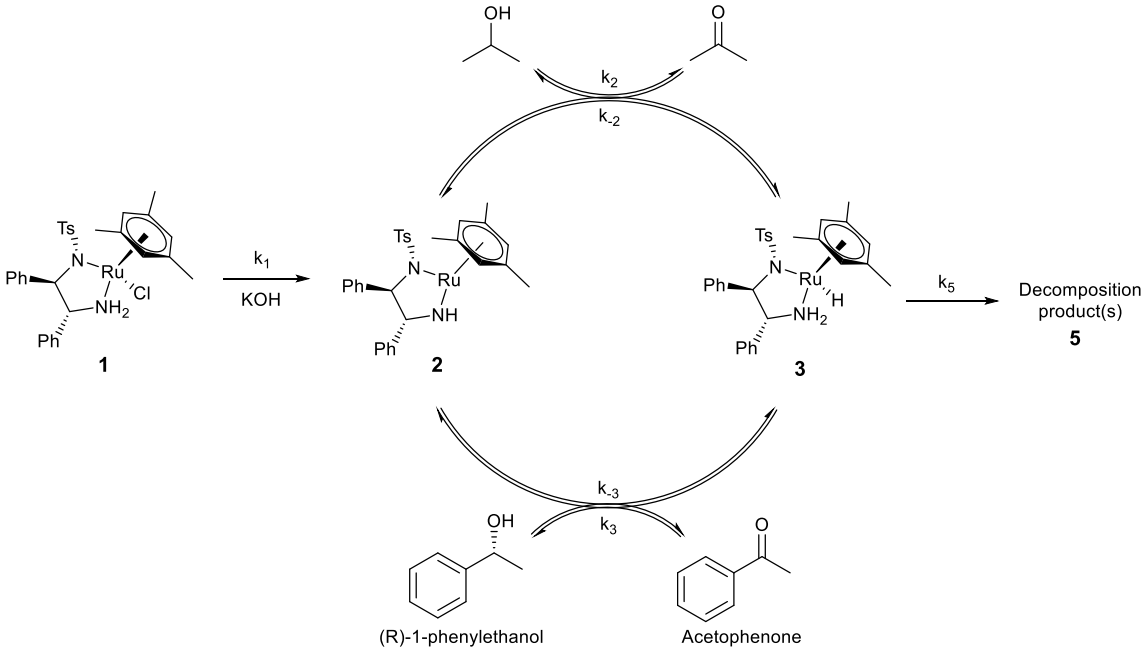

For the reaction without deactivation:

$$rate = (k_3[Acp] - k_{-3}[PE]K_{cat})\frac{[Ru]}{(K_{cat}+1)}$$

$$K_{cat} = \frac{k_{-2}[Ac] + k_3[Acp]}{k_2[IPA] + k_{-3}[PE]}$$

Since k_2, k_{-2}, k_3, k_{-3} are assumed to be independent of catalyst deactivation, the on-cycle reaction is unchanged, however the overall reaction rate decreases over time as catalyst is removed from the cycle:

Equation F: $\frac{d[Ru]_{active}}{dt} = -k_5[3]$

Equation E: $[3] = \frac{[Ru]}{(K_{cat}+1)}$

Combining Eq. E and F: $\frac{d[Ru]_{active}}{dt} = \frac{-k_5[Ru]_{active}}{(K_{cat}+1)}$

$$\int_0^t \frac{d[Ru]_{active}}{[Ru]_{active}} = -\int_0^t \frac{k_5}{(K_{cat}+1)}dt$$

$$[Ru]_{active} = [Ru]_0 \exp\left(\frac{-k_5 t}{K_{cat}+1}\right)$$

Combining this with the previously derived rate law:

$$rate = \frac{(k_3[Acp] - k_{-3}[PE]K_{cat})}{(K_{cat}+1)}[Ru]_0 \exp\left(\frac{-k_5 t}{K_{cat}+1}\right)$$

With deactivation and off-cycle species

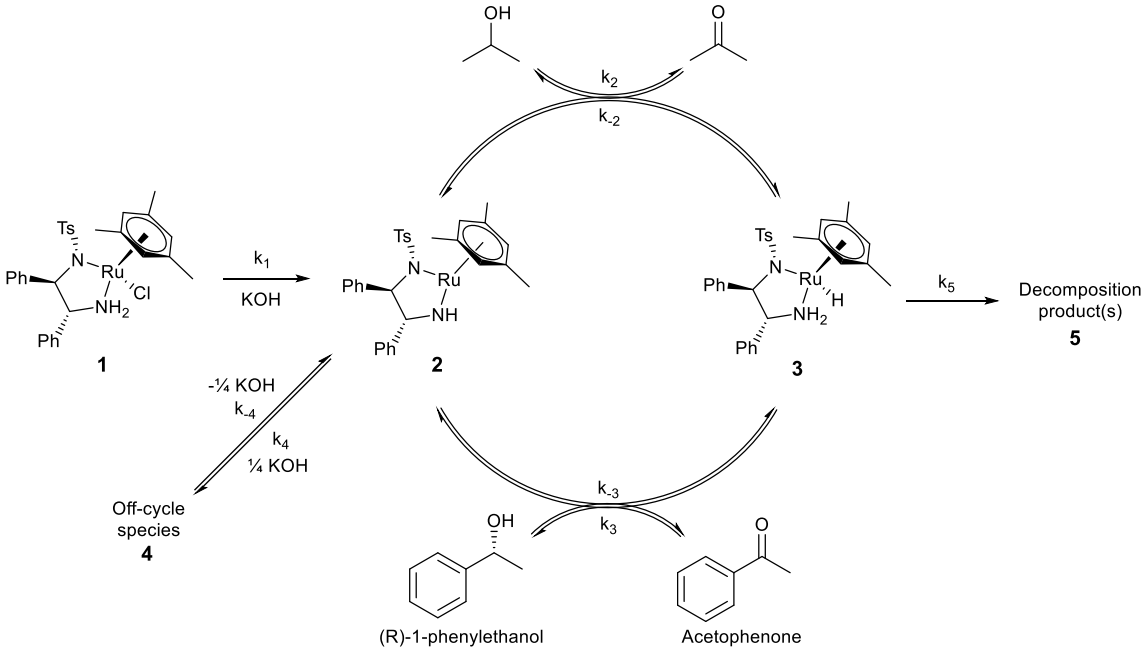

Assumptions:

- $k_1 \gg k_2$, k_{-2}, k_3, k_{-3}, therefore can be neglected and [**1**]≈0
- Steady State Approximation for on-cycle equilibria
- Quasi-equilibrium approximation for off-cycle equilibria, with inhibition constant $K_i = \frac{k_4}{k_{-4}}$
- $\frac{d[KOH]}{dt} \cong 0$

From the mechanism:

Equation A: $$rate = \frac{d[PE]}{dt} = k_3[3][Acp] - k_{-3}[2][PE]$$

Equation G: $$k_4[2][KOH]^{0.25} \cong k_{-4}[4]$$

Equation H: $$\frac{d[2]}{dt} = -k_2[2][IPA] + k_{-2}[3][Ac] + k_3[3][Acp] - k_{-3}[2][PE] - k_4[2][KOH]^{0.25} + k_{-4}[4] \cong 0$$

Equation I: $$[Ru]_{active} \cong [2] + [3] + [4]$$

Combining Eq. G and H: $$\frac{d[2]}{dt} = -k_2[2][IPA] + k_{-2}[3][Ac] + k_3[3][Acp] - k_{-3}[2][PE] - \cancel{k_{-4}[4]} + \cancel{k_{-4}[4]} \cong 0$$

Therefore the on-cycle equilibrium simplifies to that of the simple mechanism:

$$K_{cat} = \frac{k_{-2}[Ac] + k_3[Acp]}{k_2[IPA] + k_{-3}[PE]}$$ [Equation D]

Combining this with Eq. I: $$[Ru]_{active} = K_{cat}[3] + [3] + [4]$$

$$= K_{cat}[3] + [3] + \frac{k_4[2][KOH]^{0.25}}{k_{-4}}$$

$$= K_{cat}[3] + [3] + [2]K_i[KOH]^{0.25}$$

$$= K_{cat}[3] + [3] + K_{cat}[3]K_i[KOH]^{0.25}$$

$$= (K_{cat} + 1 + K_{cat}K_i[KOH]^{0.25})[3]$$

$$[3] = \frac{[Ru]_{active}}{(K_{cat}+1+K_{cat}K_i[KOH]^{0.25})} \qquad \text{[Equation J]}$$

Combining Eq. A and J: $rate = k_3[3][Acp] - k_{-3}K_{cat}[3][PE]$

$$= (k_3[Acp] - k_{-3}[PE]K_{cat})[3]$$

Equation K: $$= (k_3[Acp] - k_{-3}[PE]K_{cat})\frac{[Ru]_{active}}{(K_{cat}+1+K_{cat}K_i[KOH]^{0.25})}$$

Including catalyst deactivation:

Equation F: $$\frac{d[Ru]_{active}}{dt} = -k_5[3]$$

Combining Eq. F and J: $$\frac{d[Ru]_{active}}{dt} = -k_5\frac{[Ru]_{active}}{(K_{cat}+1+K_{cat}K_i[KOH]^{0.25})}$$

$$\int_0^t \frac{d[Ru]_{active}}{[Ru]_{active}} = -\int_0^t \frac{k_5}{(K_{cat}+1+K_{cat}K_i[KOH]^{0.25})}\,dt$$

Equation L: $$[Ru]_{active} = [Ru]_0 \exp\left(\frac{-k_5 t}{(K_{cat}+1+K_{cat}K_i[KOH]^{0.25})}\right)$$

Combining Eq. K and L gives the final rate law:

$$\boldsymbol{rate = \frac{(k_3[Acp] - k_{-3}[PE]K_{cat})}{(K_{cat} + 1 + K_{cat}K_i[KOH]^{0.25})}[Ru]_0 \exp\left(\frac{-k_5 t}{(K_{cat} + 1 + K_{cat}K_i[KOH]^{0.25})}\right)}$$

Catalyst equilibrium

From previous equations, the equilibrium between **2** and **3** may be expressed in terms of the catalyst distribution constant K_{cat}:

$$K_{cat} = \frac{[2]}{[3]} = \frac{k_{-2}[Ac] + k_3[Acp]}{k_2[IPA] + k_{-3}[PE]}$$

The stoichiometry of the reaction allows reagents and products to be expressed in terms of the overall reaction conversion, χ:

Equation M: $[PE] = [Ac]$

Equation N: $[Acp]_0 = [Acp] + [PE]$

Equation O: $[IPA]_0 = [Ac] + [IPA]$

Equation P: $[Ac] = \chi[Acp]_0$

Substituting in Eq. N and O: $K_{cat} = \frac{k_{-2}[Ac]+k_3([Acp]_0-[PE])}{k_2([IPA]_0-[Ac])+k_{-3}[PE]}$

Combining with Eq. M: $= \frac{k_{-2}[Ac]+k_3([Acp]_0-[Ac])}{k_2([IPA]_0-[Ac])+k_{-3}[Ac]}$

Combining with Eq. P: $= \frac{k_{-2}\chi[Acp]_0+k_3[Acp]_0(1-\chi)}{k_2([IPA]_0-\chi[Acp]_0)+k_{-3}\chi[Acp]_0}$

Since isopropanol is in large excess, saturation kinetics may be assumed, simplifying the expression to:

$$\boldsymbol{K_{cat} = \frac{k_{-2}\chi[Acp]_0+k_3[Acp]_0(1-\chi)}{k_2[IPA]_0+k_{-3}\chi[Acp]_0}}$$

References

1. Hall, A. M. R.; Chouler, J. C.; Codina, A.; Gierth, P. T.; Lowe, J. P.; Hintermair, U., Practical Aspects of Real-time Reaction Monitoring using Multi-nuclear High Resolution FlowNMR Spectroscopy. *Catal. Sci. Tech.* **2016,** 6, 8406-8417.

2. Hoops, S.; Sahle, S.; Gauges, R.; Lee, C.; Pahle, J.; Simus, N.; Singhal, M.; Xu, L.; Mendes, P.; Kummer, U., COPASI--a COmplex PAthway SImulator. *Bioinformatics* **2006,** 22, 3067-74.

3. Dub, P. A.; Gordon, J. C., The mechanism of enantioselective ketone reduction with Noyori and Noyori-Ikariya bifunctional catalysts. *Dalton Trans* **2016,** 45, 6756-6781.

4. Haack, K.-J.; Hashiguchi, S.; Fujii, A.; Ikariya, T.; Noyori, R., The Catalyst Precursor, Catalyst and Intermediate in the Ru(II)-Promoted Asymmetric Hydrogen Transfer between Alcohols and Ketones. *Angew. Chem. Int. Ed.* **1997,** 36, 285-288.